

On the duration of long GRBs: effects of black hole spin

A. Janiuk¹, R. Moderski¹, D. Proga²

ABSTRACT

In the frame of the collapsar model for long gamma ray bursts (GRBs), we investigate the formation of a torus around a spinning BH and we check what rotational properties a progenitor star must have in order to sustain torus accretion over relatively long activity periods. We also study the time evolution of the BH spin parameter. We take into account the coupling between BH mass, its spin parameter and the critical specific angular momentum of accreting gas, needed for the torus to form. The large BH spin reduces the critical angular momentum which in turn can increase the GRB duration with respect to the Schwarzschild BH case. We quantify this effect and estimate the GRB durations in three cases: when a hyper accreting torus operates or a BH spins very fast or both. We show under what conditions a given progenitor star produces a burst that can last as short as several seconds and as long as several hundred of seconds. Our models indicate that it is possible for a single collapse to produce three kinds of jets: (1) a very short, lasting between a fraction of a second and a few seconds, 'precursor' jet, powered only by a hyper accreting torus before the BH spins up, (2) an 'early' jet, lasting several tens of seconds and powered by both hyper accretion and BH rotation, and (3) a 'late' jet, powered only by the spinning BH.

Subject headings: accretion, accretion discs – black hole physics – gamma rays: bursts

1. Introduction

The commonly accepted mechanism for a long gamma ray burst (GRB) production invokes a collapsar scenario (Woosley 1995; Paczyński 1998; MacFadyen & Woosley 1999). In this model the material from the collapsing star feeds the accretion disk, then the accretion energy is being transferred to the jet, which in turn produces gamma rays at some distance from the central engine. Therefore the whole event cannot last much longer than the existence of a rotationally supported torus in the collapsar center. Within the collapsar model the jet can also be produced by a rotating black hole (BH) which can be spun up by the accreting torus material.

Among the most plausible mechanisms of the energy extraction from the accretion flow are the

neutrino-antineutrino annihilation (Mochkovitch et al. 1993), or the magnetic fields (e.g. Blandford & Payne 1982; Contopoulos 1995; Proga et al. 2003). The neutrino cooling (e.g. Popham, Woosley & Fryer 1999; Di Matteo et al. 2002; Janiuk et al. 2004) is effective only if the accretion rate is large ($\dot{m} \gtrsim 0.01 M_{\odot} \text{ sec}^{-1}$). Also, a large BH spin ($A_{\text{Kerr}} \gtrsim 0.9$) is thought to be a necessary condition for the jet launching: for $A_{\text{Kerr}} \sim 0.9$, about 1% of the accreted rest-mass energy is emitted back as a Poynting jet (Blandford & Znajek 1977; McKinney 2005).

On the other hand, the rotationally supported torus may form only when the substantial amount of specific angular momentum is carried in the material. In our recent article (Janiuk & Proga 2008; hereafter Paper I) we studied the problem of whether the collapsing star envelope contained enough specific angular momentum in order to support the formation of the torus. This condition was parametrized by the so called critical specific angular momentum which in case of a non-rotating BH depends only on its mass. In the present work,

¹Copernicus Astronomical Center, Bartycka 18, 00-716 Warsaw, Poland

²University of Nevada, Las Vegas, 4505 Maryland Pkwy, NV 89154, USA

we take into account also the BH rotation and the coupling between the specific angular momentum of the accreting material, the BH mass and its spin.

We show that as in Paper I, during the collapse the amount of the rotating material, which was initially available for the torus formation, may later become insufficient to support the torus. Moreover, the spin of the BH is changed by accretion (see e.g. recent studies by Gammie et al. 2004; King & Pringle 2006; Belczyński et al. 2007). In our models, depending on the accretion scenario, both the spin-up and spin-down of BH are possible, because part of the infalling material has very small specific angular momentum.

The outline of this paper is as follows. In Section 2, we briefly describe the model of the evolution of the collapsing star together with the initial conditions. The results are presented in Section 3; the GRB durations are estimated in Section 3.3. In Section 4, we discuss results in the context of a long GRB production mechanisms and conditions for the distribution of the specific angular momentum in a progenitor star. In Appendix A we provide some formulae for the description of the mass and spin evolution of the BH.

2. Model

The model is essentially the same as in Paper I, with one important modification, namely the evolution of the spin of the BH. As the initial conditions, we use the spherically symmetric model of the $25.6 M_{\odot}$ pre-supernova (Woosley & Weaver 1995). The density and mass profiles were shown in Figure 1 of Paper I. The mass of the iron core is equal to 1.7 solar masses, while the envelope mass, equal to $23.9 M_{\odot}$, is available for accretion.

The distribution of the specific angular momentum within a star is parametrized as either a function of the polar angle θ (model **A**), or a function of both radius r and θ (model **D**). In Paper I, we considered two more models, i.e., those named **B** and **C**, but they did not differ significantly from models **A** and **D**, respectively. Therefore we focus here only on the two models.

In model **A**, we assume the specific angular momentum, l_{spec} , to depend only on the polar angle:

$$l_{\text{spec}} = l_0 f(\theta), \quad (1)$$

where

$$f(\theta) = 1 - |\cos \theta|. \quad (2)$$

The normalization, l_0 , of this dependence is defined with respect to the critical specific angular momentum, l_{crit} , for the seed BH:

$$l_{\text{crit}}(M, A) = \frac{2GM}{c} \sqrt{2 - A + 2\sqrt{1 - A}}, \quad (3)$$

so that $l_0 = x l_{\text{crit}}$, where x is a free parameter. In the Eq. 3, M is the initial BH mass (iron core mass) and $A \equiv A_{\text{Kerr}}$ is its initial dimensionless spin parameter (see Appendix A).

In model **D**, we assume that the specific angular momentum depends on the polar angle, as well as on the radius in the envelope, as:

$$l_{\text{spec}} = l_0 g(r) f(\theta), \quad (4)$$

where

$$g(r) f(\theta) = \sqrt{\frac{r}{r_{\text{in}}}} \sin^2 \theta, \quad (5)$$

r_{in} is the inner radius of the envelope, and l_0 is given below the Eq. 3.

The model **D** corresponds to a constant ratio between the centrifugal and gravitational forces. Note that the strong increase of l_{spec} with radius will lead to a very fast rotation at large radii. Therefore, a cut off may be required at some maximum value, l_{max} (Section 3.2).

The normalization of the models is chosen such that the specific angular momentum is always equal to the critical value at $\theta = 90^\circ$ (and at $r = r_{\text{in}}$ if the model depends on radius). In Section 3, we present the results of our calculations considering a range of x .

Initially, the mass of the BH is given by the mass of the iron core of the star, $M = M_{\text{core}}$. The initial conditions for the torus formation in the collapsar are such that only a fraction of the envelope mass carries the specific angular momentum larger than the (initial) critical value. As shown in Eq. 3, l_{crit} is defined by the mass of BH, M , and its spin, A_{Kerr} . However, as the collapse proceeds, the mass of BH will increase and also its spin will change (increase or decrease, depending on the accretion scenario). Therefore the critical specific angular momentum will be changing as well.

To compute the mass of the part of the envelope that has specific angular momentum large enough

to form a torus around a given BH, and to estimate the time duration of the GRB powered by accretion, we need to know the BH mass and spin.

We assume that at each step of the evolution the BH grows by accreting a mass Δm^k :

$$M^k = M^{k-1} + \Delta m^k, \quad (6)$$

and that the BH angular momentum changes as:

$$J^k = J^{k-1} + \Delta J^k. \quad (7)$$

Here the increment of mass of BH is :

$$\Delta m^k = 2\pi \int_{r_k}^{r_k + \Delta r_k} \int_0^\pi \rho(r, \theta) r^2 \sin \theta d\theta dr, \quad (8)$$

and the accreted angular momentum is:

$$\Delta J^k = 2\pi \int_{r_k}^{r_k + \Delta r_k} \int_0^\pi \min(l(r, \theta), l_{\text{crit}}(M, A)) \rho(r, \theta) r^2 \sin \theta d\theta dr. \quad (9)$$

In the above equation we take into account the fact that the angular momentum larger than l_{crit} is not accreted onto the BH, but transported outwards. In this way we provide the physical condition for the spin parameter, which must always be $A_{\text{Kerr}} \lesssim 1.0$. (However, we do not specify any particular mechanism(s) responsible for the angular momentum transport.)

The new spin parameter will then be equal to:

$$A^k = \frac{cJ^k}{G(M^k)^2}. \quad (10)$$

In the next step of the iteration, both the new parameter and new mass of BH will affect the critical specific angular momentum. Now, depending on the accretion scenario, the part of the envelope material determined by the new l_{crit} , will accrete onto BH.

We consider here three possible accretion scenarios:

1. the accretion onto BH proceeds at the same rate both from the torus and from the gas close to the poles (uniform accretion);
2. the envelope material with $l < l_{\text{crit}}^k$ falls on the BH first. Thus, until the polar funnel is evacuated completely, only this gas contributes to the BH mass. After that, the material with $l > l_{\text{crit}}^k$ accretes;

3. the accretion proceeds only through the torus, and only this material contributes to the BH growth. In this case the rest of the envelope material is kept aside until the torus is accreted.

The above iterative procedure and the accretion scenarios were described in Paper I and illustrated in Figure 2 there. The main modification in the present work is the non-zero spin parameter of BH, which leads to a different initial condition for l_{crit} and more complex evolution of the collapsar. Now l_{crit} is coupled to both the BH mass M and the spin parameter A_{Kerr} .

Due to the increasing BH mass and its changing spin, the critical angular momentum also changes. We always stop the calculations, when there is no material with $l > l_{\text{crit}}^k$, i.e. able to form a torus. However, in a real situation the GRB prompt phase will be stopped earlier, i.e. if the free fall timescale is too large, or the accretion rate is too small, to be adequate to power the GRB ($\dot{m} = 0.01 - 1.0 M_\odot \text{ s}^{-1}$). Also, in the present model it is important that the BH spin parameter is large during the GRB emission.

The duration of the GRB is estimated as the ratio between the mass accreted through the torus, and the accretion rate \dot{m} :

$$T_{\text{GRB}} = \frac{M_{\text{accret}}^{\text{torus}}}{\langle \dot{m} \rangle}, \quad (11)$$

assuming that the GRB prompt emission is equal to the duration of the torus replenishment. The accretion rate, \dot{m} depends on time and we determine it instantaneously during the iterations by the free fall velocity of gas in the torus. Finally, we impose the conditions for a minimum accretion rate and the minimum spin parameter. We then estimate the GRB duration as the ratio between the total mass accreted in the torus and the mean accretion rate.

3. Results

3.1. Models with the specific angular momentum dependent on θ

In this Section, we present the results for model **A** of the specific angular momentum distribution in the collapsing star, and for different accretion scenarios: (1), (2), and (3). The models are hereafter labeled as **A1**, **A2** and **A3**. In this model,

l_{spec} does not depend on radius, but only on the polar angle, θ . The normalization of this distribution, $x = l_0/l_{\text{crit}}$, is a free parameter of our model, and the results are presented as either a function of x , or for some chosen, exemplary values of x .

First, we study how much mass can be accreted onto the BH during the collapse, both in total and through the rotating torus, as long as such a torus exists. This, in the first approximation, will give an estimate of the GRB duration, because it is proportional to the amount of material which is available for accretion.

The Figure 1 shows the mass accreted onto the BH, as a function of x . Left panel of this Figure shows the scenario **A1**, in which the mass accretes uniformly. The thick solid line is for the total accreted mass, and the thinner line is for this fraction of mass, which has been accreted through the torus. The single dashed line shows the scenario **A3**, in which the mass accretes only through the torus. We see, that in the model **A3**, the accreted mass can be larger than in the model **A1** (for $x \leq 8$), although the accretion in the model **A3** proceeds only through the torus. This is because in model **A3**, the BH spin can only increase, which in turn lowers the value of l_{crit} , making the condition for $l_{\text{spec}} > l_{\text{crit}}$ easier to be satisfied. Although at the same time the growing BH mass makes the l_{crit} increase, for small x this effect is less than the effect of the BH spin. In model **A1**, the BH spin decreases (see below), so both the decreasing spin and increasing BH mass affect l_{crit} in the same way.

The right panel of the Figure 1 shows the scenario **A2**, in which the matter accretes onto the BH first from the poles, and then through the torus. In this scenario, for $x < 7$, there is no torus accretion. This is because the condition for $l_{\text{spec}} > l_{\text{crit}}$ is never satisfied after the polar material has accreted onto the BH. The total mass accreted is that from the poles. Only for $x > 7$, some fraction of the envelope material is still capable of forming the torus and accretes through it (thin line). This mass adds to the total accreted mass (thick line).

All the results shown here are for a rotating BH (the initial Kerr parameter was assumed $A_0 = 0.85$ and in all the models we had $A_{\text{Kerr}} > 0$ throughout the collapse; see below). In general, the mass accreted onto the spinning BH was larger

than in the case of the non rotating BH, studied in Paper I. For instance, for $x = 10$, it is about $15.5 M_{\odot}$ and $15 M_{\odot}$ (model **A1**, total accreted mass), $8 M_{\odot}$ and $7 M_{\odot}$ (model **A1**, torus accreted mass), and $14 M_{\odot}$ and $12 M_{\odot}$ (model **A3**), for a rotating and non-rotating BHs, respectively.

The above results can be understood, when we study the evolution of the critical specific angular momentum during the collapse, as shown in Figure 2. The Figure shows l_{crit} as a function of radius. For the scenario **A1**, the accretion is uniform and the result depends only weakly on x . However, for small x the calculations were stopped earlier, when the torus ceased to exist. For scenario **A3**, the results depend on x . For smaller x , the torus mass is smaller, and therefore less material may accrete onto the BH. Because the BH is less massive, the increase of l_{crit} is slower. Obviously, the opposite is true in scenario **A2** shown in the right panel of the Figure 2 (only the first phase of polar accretion is shown, for clarity).

Of course, these results are affected by the large, and changing, Kerr parameter, A_{Kerr} . Because the term under the square root in the Eq. 3 is a decreasing function of A_{Kerr} , the models with a rotating BH always result in a smaller critical angular momentum than for the non-rotating BH. Therefore the conditions for the torus existence in the former models can be satisfied more easily, and one could expect that the GRB prompt emission can last longer than we found in Paper I.

The Figure 3 shows the evolution of A_{Kerr} during the collapse, for scenarios **A1** and **A3** in the left panel, and for scenario **A2** in the right panel. In the uniform accretion scenario **A1**, the BH first spins up, and then spins down. Here, the spin evolution depends strongly on x . In scenario **A2**, BH spins down during the polar accretion phase, and the larger x , the smaller is the final spin. Then, during the second phase of the model **A2**, i.e. during the torus accretion, the BH spins up very quickly, up to $A_{\text{Kerr}} = 0.9999$. The latter is not shown in the right panel of the Figure 3 for clarity. In the left panel, the dashed lines mark results for the torus accretion scenario **A3**, where the final spin is always at $A_{\text{Kerr}} = 0.9999$ and only initially, very weakly, depends on x .

We note here that the BH spin never reaches $A_{\text{Kerr}} = 1.0$ and only approaches this value asymptotically. The result of $A_{\text{Kerr}} = 1.0$ would be un-

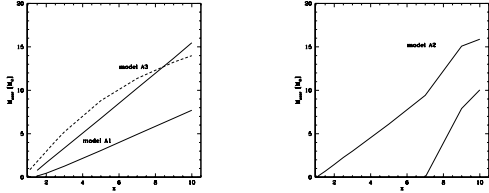


Fig. 1.— The mass accreted onto BH during the collapse, in model A for the angular momentum distribution. Left panel: The uniform accretion scenario (A1, solid lines). The two lines represent the total accreted mass (thick line) or the mass accreted through the torus (thin line). The torus accretion scenario (A3) is shown by the dashed line. Right panel: The accretion scenario A2, showing the total accreted mass (thick line) and the mass accreted through the torus (i.e. in the phase 2; thin line).

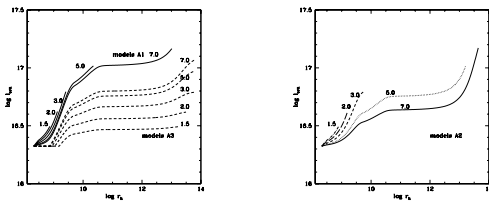


Fig. 2.— The critical specific angular momentum during the collapse, i.e. as a function of radius r_k (the current inner radius of the envelope as it keeps accreting onto BH). Left panel: The solid lines show the uniform accretion scenario (A1), while the dashed lines show the torus accretion scenario (model A3), for a range of normalizations of the specific angular momentum: $x=1.5, 2.0, 3.0, 5.0$ and 7.0 , marked on the right for each curve. Right panel: The accretion scenario A2 (only phase 1), for the same normalizations x .

physical, while the limit of $A_{\text{Kerr}} \lesssim 1.0$ is naturally provided by our model, in which only the specific angular momentum of $l_{\text{spec}} \leq l_{\text{crit}}$ contributes to the BH spin.

The evolution of the BH spin is summarized again in the Figure 4. Here we plot the final value of A_{end} , as a function of x . As the Figure shows, A_{end} can be less than the initial value of $A_0 = 0.85$ for models **A1** and **A2**. In other words, the effective spin down of the BH is possible either for the uniform accretion, **A1**, but with a small normalization parameter x , or in the two stage accretion, **A2**, but when the normalization x is so small that the rotating torus is unable to form. In other models, the BH is either effectively spun-up, to $A_{\text{Kerr}} = 0.9999$ (model **A3**), or the final spin does not differ much from the initial one (model **A1**, large x).

We checked that these results only very weakly depend on the assumed A_0 . For $A_0 = 0.75$ and $A_0 = 0.95$, the final distribution of A_{end} with x is also very close to that for $A_0 = 0.85$. Interestingly, this means that in case of initially rapidly spinning BH with $A_0 = 0.95$, the object is always effectively spun-down by the uniform accretion.

3.2. Models with the specific angular momentum dependent on r and θ

Now, we investigate how the total accreted mass and in consequence the duration of the GRB will be affected if l_{spec} in the collapsing star is given by a fixed ratio of the centrifugal to the gravitational force. We discuss here the model **D** for the l_{spec} distribution, and the three accretion scenarios are referred to as **D1**, **D2** and **D3**.

In this model, the specific angular momentum is a strong function of radius. Therefore, in a realistic situation we must have a maximum value of the specific angular momentum, l_{max} . Here we adopt a moderate value of $l_{\text{max}} = 10^{17} \text{ cm}^{-2} \text{ s}^{-1}$, following MacFadyen & Woosley (1999) and Proga et al. (2003). The Figure 5 shows the mass accreted onto the BH in three accretion scenarios (**D1** and **D3** in the left panel and **D2** in the right panel). Contrary to what was found in Paper I, the accreted mass is constant with x only for the torus accretion scenario **D3**, while in models **D1** and **D2** it depends on x . This is because the critical specific angular momentum depends now not only on the

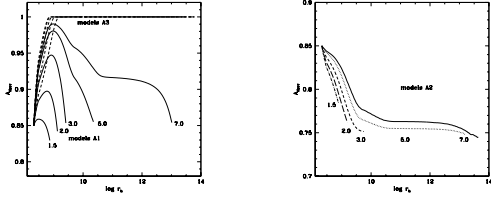


Fig. 3.— The BH spin parameter during the collapse, i.e. as a function of radius r_k (the current inner radius of the envelope as it keeps accreting onto BH). Left panel: The solid lines show the uniform accretion scenario (A1), while the dashed lines show the torus accretion scenario (model A3), for a range of normalizations of the specific angular momentum: $x=1.5, 2.0, 3.0, 5.0$ and 7.0 , marked on the right for each curve. Right panel: The accretion scenario A2 (only phase 1), for the same normalizations x .

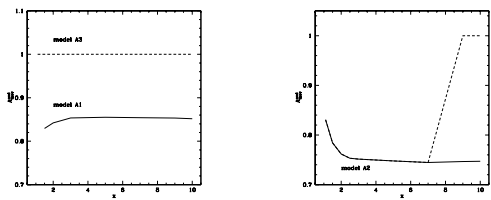


Fig. 4.— The final BH spin parameter after the collapse. Left panel: models of the uniform accretion (A1, solid line), and torus accretion (A3, dashed line), as a function of the initial normalization of the specific angular momentum. Right panel: The accretion scenario A2, first phase of polar accretion (solid line) and second phase of torus accretion (dashed line).

BH mass but also on the spin parameter. The BH spin is changing during the collapse in models **D1** and **D2**, because the accreting material is not only that from the torus (i.e. $l_{\text{spec}} > l_{\text{crit}}$, which does not influence the BH spin), but also that from the poles. The rate of change of the BH spin strongly depends on x , as we show in Figs. 6 and 7.

The Figure 6 shows the BH spin parameter, A_{Kerr} , as a function of radius during the collapse, and the Figure 7 shows the final spin $A_{\text{Kerr}}^{\text{end}}$. When the torus accretes, similarly to model **A3**, in the model **D3** the BH is spinning up to $A_{\text{Kerr}} = 0.9999$. However, in the uniform accretion model **D1**, the BH is effectively spun down for most normalizations, i.e. $x < 7$. For very small x , it is even possible for the BH to spin down almost completely at the end of the collapse. The same is true for the first phase of the scenario **D2**, i.e. the polar accretion. The existence of a torus in the second phase is possible only for $x > 0.7$ and in this case the BH finally spins up to $A_{\text{Kerr}} = 0.9999$. For $x \geq 0.7$ in models D1 and D2, the BH spin slightly fluctuates. This is because of the density profile in the accreting envelope, which is not perfectly smooth, but consists of layers, in which various heavy elements are dominant. In models **D**, the specific angular momentum is a function of radius, which makes the angular momentum accreted onto the BH much more sensitive to the position of the current shell, than in case of models **A**. As a result, for some layers the BH may accrete more mass than the angular momentum, and A_{Kerr} decreases, while for some other layers the BH obtains more angular momentum than mass, and A_{Kerr} increases (see Eq. 8 and 9). This is not the case for the model **D3**, because here the angular momentum that contributes to the BH spin is always given by l_{crit} .

3.3. Duration of a GRB

In the first approximation, the duration of a GRB may be proportional to the mass accreted via the torus during the collapse (as shown in Figures 1 and 5). However, as the accretion rate is not constant, the torus accretion will depend also on the accretion rate (see Eq. 11).

The Figure 8 shows the instantaneous accretion rate during the collapse, i.e. as a function of the current inner radius of the envelope, as it keeps accreting onto the BH. In models **A1**, **A2** and

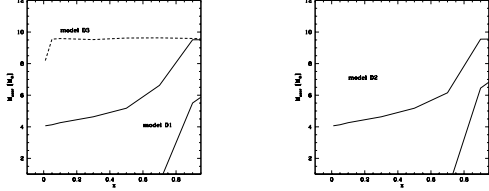


Fig. 5.— The mass accreted onto BH during the collapse, i.e. as a function of radius r_k (the current inner radius of the envelope as it keeps accreting onto BH). The plots show model D for the angular momentum distribution. Left panel: The uniform accretion scenario (D1, solid line) is presented by the two lines representing the total accreted mass (thick line) and the mass accreted through the torus (thin line). The torus accretion scenario (D3) is shown by the dashed line. Right panel: The accretion scenario D2, showing the total accreted mass (thick line) and the mass accreted through the torus (i.e. in the phase 2; thin line).

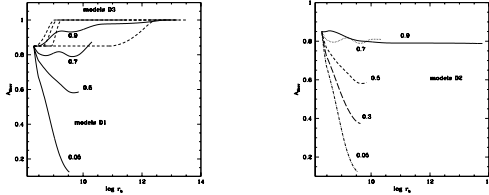


Fig. 6.— The BH spin parameter during the collapse, i.e. as a function of radius r_k (the current inner radius of the envelope as it keeps accreting onto BH). Left panel: The solid lines show the uniform accretion scenario (D1), while the dashed lines show the torus accretion scenario (model D3), for a range of normalizations of the specific angular momentum: $x = 0.05, 0.5, 0.7$ and 0.9 , marked on the right for each curve. Right panel: The accretion scenario D2, for the same normalizations x .

A3, the torus exists from the very beginning of the collapse, and then the accretion rate is the largest, equal about $0.08-0.15 M_\odot \text{ s}^{-1}$, depending on x . Later, as the outer shells accrete, the accretion rate drops and for all the models it is less than $0.01 M_\odot \text{ s}^{-1}$ at $\log r = 8.8-9.8$, depending on x .

In models **D1**, **D2** and **D3**, the torus formation is delayed, because the faster rotating shells are in the outer parts of the envelope. For large x , the torus is formed already for $\log r \sim 8.4-9.0$, where the free-fall time scale is very short and the accretion rate is large, on the order of $0.02-0.04 M_\odot \text{ s}^{-1}$. For small x (i.e. $x < 0.7$ for model **D1** and $x < 0.3$ for model **D3**), the torus does not form until the outermost shells accrete, and therefore the maximum accretion rates obtained in these models are always below $0.01 M_\odot \text{ s}^{-1}$.

This will have important implications, because as shown in a number of studies of the hyperaccreting tori in the GRB central engine, for the accretion rates smaller than about $0.01 M_\odot \text{ s}^{-1}$ the neutrino cooling becomes inefficient (see e.g. Popham, Woosley & Fryer 1999; Di Matteo et al. 2002; Janiuk et al. 2004). Therefore it is reasonable to limit our definition of an 'active' central engine to such a minimum accretion rate.

Another limitation for an efficient central engine will be the minimum spin of the BH. Here we assume a conservative value of $A_{\min} = 0.9$, to provide the energy source for the jet (McKinney 2005). The Figure 9 shows the duration of the central engine activity as a function of x , for both models **A** and **D** and for all the 3 accretion scenarios. The plots account for the central engine activity time, when both assumptions are satisfied, i.e. the accretion rate must be larger than \dot{m}_{\min} and the BH spin must be larger than A_{\min} .

As the Figure shows, the torus accretion scenario, marked with a dashed line, leads to the longest duration of a GRB: up to 50 seconds in model **A3** and up to 130 seconds in model **D3**. In this scenario, the BH spin is always larger than our minimum value, and in most cases the BH was spun up to $A_{\text{Kerr}} = 0.9999$. Therefore in practice, what determines the GRB duration in this case, is the accretion rate. Consequently, the model **A3**, in which the accretion rate is larger, results in shorter GRBs than the model **D3**.

The uniform accretion scenario leads to a

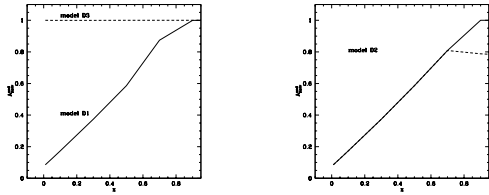


Fig. 7.— The final BH spin parameter after the collapse. Left panel: models of the uniform accretion (D1, solid line), and torus accretion (D3, dashed line), as a function of the initial normalization of the specific angular momentum. Right panel: The accretion scenario D2, first phase of polar accretion (dashed line) and second phase of torus accretion (solid line).

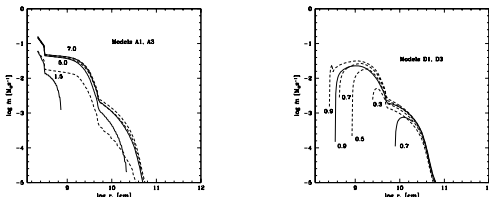


Fig. 8.— The instantaneous mass accretion rate during the collapse, i.e. as a function of radius r_k (the current inner radius of the envelope as it keeps accreting onto BH). The plots show 2 models and 3 exemplary values of the normalization parameter x . Left: $x = 7.0, 5.0$ and 1.5 (marked by numbers); solid lines mark the accretion scenario (1) and dashed lines mark scenario (3). Right: $x = 0.7, 0.5$ and 0.05 (marked by numbers); scenarios (1) - solid lines; scenario (3) - dashed lines.

shorter GRB than in case of a torus accretion. Now, also the condition for a minimum BH spin is important, because for some models the BH has not spun up or has been spun down, below $A_{\text{Kerr}} = 0.9$. In the model **A1**, for very small x , no GRB was produced. Moreover, in model **D1** the GRBs occurred only for $x > 0.7$ (neither the spin nor the accretion rate condition was satisfied for smaller x), and the longest GRB duration was $T \approx 100$ s.

The shortest GRBs were produced by scenario (2), i.e. the two phase accretion (obviously, only in these models which had the second phase with a torus accretion). In models **A2** and **D2**, the activity of the GRB central engine was never longer than 50 seconds.

The Figure 9 shows the duration of a GRB resulting from the assumption of a minimum accretion rate *and* the minimum BH spin. However, as we discuss below in Section 4, these two conditions refer to the two various mechanisms of powering the jet, which is emitting the gamma rays. The time T_{GRB} is different, if we consider only one of these mechanisms, i.e. impose only one of the above conditions. For instance, if we took into account only the condition for a minimum BH spin, in model **A3** the GRB was up to 4 times longer than that presented in the left panel of Fig. 9. Also, the model **D3** produced long GRBs powered only by the BH spin, for which the minimum accretion rate condition was not satisfied (the models with $x < 0.3$). The very long GRB durations for the spin condition result from the fact that at the end of the collapse, the BH is still spinning fast, while the accretion rate is very small and the mass accreted through the torus is large. On the other hand, taking into account only the condition for the accretion rate, regardless of the BH spin, led to somewhat shorter (sometimes even two times shorter) GRBs than these presented in Fig. 9. This comes from the fact that the largest accretion rate, leading to a shorter GRB, is always at the beginning of the collapse, when the BH has not yet spun up enough.

4. Discussion and conclusions

In this article, we studied the collapsar model for long GRBs, powered by accretion onto a spinning BH, which formed from the core of a mas-

sive, rotating Wolf-Rayet star. To describe the rotation of the stellar interior, we adopted two different analytical functions, accounting for either a differential rotation (models **A1**, **A2**, **A3**), or a constant ratio between the gravitational and centrifugal forces (models **D1**, **D2**, **D3**). This study is an important test for the rotation models of the GRB progenitor stars (e.g. Heger et al. 2005; Yoon et al. 2006; Detmers et al. 2008).

To describe how the accretion proceeds during the collapse, we adopted three different scenarios: (1) uniform accretion, (2) two phase accretion, first from the poles and then from the torus and (3) only torus accretion. The accretion onto the BH is in our approach a homologous process, in which the subsequent shells of the envelope add their mass to the central object. The angular momentum is also accreted, but the limit for it is the critical angular momentum, to prevent the BH from spinning with $A_{\text{Kerr}} \geq 1.0$. In this sense, we assume that the whole angular momentum with $l > l_{\text{crit}}$, i.e. in the torus, is transported outwards. We do not invoke any particular mechanism of transport (i.e. the viscosity), and the momentum is taken out by a negligibly small amount of mass (e.g., Pringle 1981). This simplified approach describes well a more realistic situation, in which the matter with small and large angular momentum can be mixed. Therefore some parts of the gas with large l_{spec} might reach the BH, while some other parts might be blown out with the polar outflow.

We focused on the evolution of the BH spin during the collapse. The large BH spin is important for GRB production in two ways: first, to power the jet emission via the Blandford-Znajek (BZ) mechanism, and second, because it alters the condition for the torus formation, i.e. the critical specific angular momentum. We found that the spin of the BH strongly depends on both the model of the l_{spec} distribution and on the accretion scenario.

In the torus accretion (i.e. either the second phase of the scenario 2, models **A2** and **D2**, or the scenario 3, models **A3** and **D3**), the accreting material has specific angular momentum always $l_{\text{spec}} \geq l_{\text{crit}}$. This angular momentum must be transported outwards before reaching the BH, so that the gas which is changing the BH spin has the specific angular momentum equal to l_{crit} .

Nevertheless, it is enough to spin up the BH to the maximal rotation, $A_{\text{Kerr}} = 0.9999$, which happens in most cases at the very beginning of the collapse. The polar accretion, i.e. the first phase of scenario 2. (models **A2** and **D2**), leads only to the BH spin-down in all the models. The uniform accretion scenario is the most complex. In the model **A1** it leads only to a temporary increase of the BH spin, while during the accretion of the outer shells, the BH is spinning down. In the model **D1**, the BH spin first decreases, while later during the collapse it may increase, provided the stellar envelope contains enough l_{spec} .

We found that in model **A1**, the final BH spin after the collapse is always about $A_{\text{end}} \sim 0.85$, and it does not depend on the normalization the specific angular momentum contained in the stellar envelope, i.e. on x . However, the pattern of the BH spin evolution is very sensitive to this parameter. Therefore for small values of x it may happen that even for a short time during the collapse, the BH never reaches a spin $A_{\text{Kerr}} > 0.9$, which we consider necessary to power the jet with the BZ mechanism. However, in the same models, the torus does exist and the accretion rate in the torus is large enough to power the jet via the neutrino annihilation. This might lead to a relatively short living (less than $\sim 7-8$ s) GRB central engine without a very rapidly spinning BH. On the other hand, for $A_{\text{Kerr}} > 0.9$, the stage of a rapidly spinning BH begins very shortly after the collapse has started, and lasts much longer after the accretion rate in the torus has dropped below $\dot{m} = 0.01 M_{\odot} \text{s}^{-1}$. For instance, a GRB powered by the BZ mechanism may last almost ~ 120 s, while that powered by the neutrino annihilation (concurrent with the spinning BH) lasted only ~ 40 s. A very short time required for the BH to spin up, while the collapse proceeds, is of the order of ~ 1.5 s.

In model **D1** the situation is different. Here we do not find any models with only the neutrino-powered bursts, i.e. with a large accretion rate but not accompanied with a rapidly spinning BH. In other words, whenever there exists a torus with a large accretion rate, the BH is spun up to $A_{\text{Kerr}} > 0.9$, and the timescale for this spin up is a fraction of a second (~ 0.15 s). Similarly to model **A1**, the stage of a large BH spin can last much longer, after the accretion rate has dropped below $\dot{m} = 0.01 M_{\odot} \text{s}^{-1}$. For instance, the BZ-powered burst

lasting ~ 430 s is accompanied by a ~ 100 s burst powered by both BZ and neutrino mechanisms.

Observationally, this behavior may have led to three kinds of jets. The first is a very short, lasting between a fraction of a second and few seconds, 'precursor' jet, powered by only the neutrino annihilation, before the BH spins up. The second is an 'early' jet, lasting several tens of seconds and powered by both neutrino and BZ mechanisms. The third is a 'late' jet, powered by only the spinning BH via the BZ mechanism. In our models, we can have the GRB jets with all the three components, as well as the 'orphan precursor' jets, when the BH failed to spin up.

The precursors have been detected by Ginga, BeppoSAX, BATSE, INTEGRAL and Swift in some GRBs (e.g. Murakami et al. 1991; Piro et al. 2005; Lazzati 2005; Romano et al. 2006; McBreen et al. 2006). These GRB precursors are an important observational test for their theoretical models (e.g. Ramirez-Ruiz et al. 2002; Umeda et al. 2005; Morsony et al. 2007; Wang & Meszaros 2008). For instance, in the sample of BATSE bursts, studied by Lazzati (2005), about 20% of the bursts had a precursor, which was characterized by a non-thermal spectrum and contained less than 1 per cent of the total counts. The main GRB in these events was delayed with respect to the precursor by 10-200 seconds. As argued by Morsony et al. (2007), who in the 2-D numerical MHD simulations identified three distinct phases during the jet propagation, this large gap in the emission might be a selection effect. Because of different opening angles of these three jets, some observers located at large viewing angles may see a 'dead' phase, i.e. the break in the emission, related to the second jet. Another explanation of the gap between the precursor and the main jet could be the development of the instabilities in the hyper-accreting disk (Perna et al. 2006; Janiuk et al. 2007), possibly combined with the viewing angle effects.

We therefore conclude that in the present model, the 'dead' phase would refer to an 'early' jet, which is powered by both neutrino and BZ mechanisms and can be collimated to a much narrower angle than the 'late' jet. For the viewing angle larger than the 'early' jet but smaller than the 'late' jet opening angle, the observer should see the precursor, followed by a gap in the emission on the order of 40-150 seconds, and then see

the 'main' GRB. We also notice that recently, the observation of the bright, long GRB 080319B (Racusin et al. 2008), seems to have confirmed that the jet's opening angle may vary, indicating for the two types of jets.

Finally, comparing our current models with the results presented for a non-rotating BH (Paper I), we notice that the GRB durations are similar in case of model **A1**, i.e. ~ 40 s vs. ~ 50 for the Schwarzschild and Kerr BH main jet, respectively. In model **D1**, the discrepancy is more pronounced, namely ~ 50 s vs. ~ 100 s, respectively. On the other hand, in the current work, the model **D1** produces GRBs powered by neutrino annihilation only for a very narrow range of parameters (i.e. x), while in Paper I for this model we found no limitations for x .

This work was supported in part by grant 1P03D00829 of the Polish State Committee for Scientific Research, the Polish Astroparticle Network grant 621/E-78/SN-0068/2007 and NASA under grant NNG05GB68G.

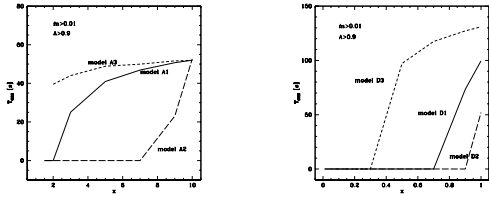


Fig. 9.— The total duration of a GRB. Left panel: models **A** for the specific angular momentum distribution; Right panel: models **D**. The three accretion scenarios are uniform accretion (A1, D1; solid lines), polar and then torus accretion (A2, D2; long dashed lines) and torus accretion (A3, D3; short dashed lines). The plots are in the function of the initial normalization of the specific angular momentum. The calculated time T_{GRB} results from the assumption of a minimum accretion rate, $\dot{m}_{min} = 0.01 M_{\odot} s^{-1}$, and the minimum BH spin of $A_{min} = 0.9$. This time refers to the 'early' jet; see Sec. 4.

A. Spin evolution

Space-time around astrophysical BHs is described by the Kerr metric with two parameters, the mass-energy M , and the angular momentum J . Below we use dimensionless angular momentum $A \equiv cJ/GM^2$ and dimensionless radius $\bar{r} = rc^2/GM$.

The change of BH parameters due to accretion of rest mass dm is given by (Moderski & Sikora 1996; see also Moderski et al. 1998):

$$c^2 dM = e dm, \quad (\text{A1})$$

$$dJ = l dm, \quad (\text{A2})$$

where e and l are the specific energy and angular momentum of accreted matter, respectively.

Combination of equations (A1) and (A2) gives the evolution equation for the BH spin:

$$\frac{dA}{d \ln M} = \frac{\bar{l}}{\bar{e}} - 2A, \quad (\text{A3})$$

where dimensionless quantities $\bar{l} \equiv cl/GM$ and $\bar{e} \equiv e/c^2$ can be functions of A . Thus whether spin increases or decreases depends on the sign of the expression $\bar{j} - 2A\bar{e}$.

A.1. Geometrically thick disk

We will consider an accretion from geometrically thick disc as an example. In such a case the inner edge of the accretion disc is located at the marginally bound orbit, r_{mb} and

$$\bar{r}_{mb} = 2 \mp A + 2(1 \mp A)^{1/2} \quad A = \pm \bar{r}_{mb}^{-1/2} (2 - \bar{r}_{mb}^{1/2}) \quad (\text{A4})$$

$$\bar{e}_{mb} = 1 \quad (\text{A5})$$

$$\bar{l}_{mb} = 2\bar{r}_{mb}^{1/2} \quad (\text{A6})$$

where upper signs are for direct accretion, while lower signs are for retrograde accretion, respectively.

The solution of equation (A3) is (Abramowicz & Lasota 1980):

$$\bar{r}_{mb} M^2 = \bar{r}_{mb0} M_0^2, \quad (\text{A7})$$

where \bar{r}_{mb0} is the initial marginally bound orbit.

From equations (A7) and (A4) we obtain

$$A = \begin{cases} \pm \frac{\bar{r}_{mb0} M_0}{M} (2 - \frac{\bar{r}_{mb0} M_0}{M}) & \text{for } \frac{M}{M_0} \leq \sqrt{\bar{r}_{mb0}} \\ \pm 1 & \text{for } \frac{M}{M_0} \geq \sqrt{\bar{r}_{mb0}} \end{cases}, \quad (\text{A8})$$

where, for a given A_0 , the value of \bar{r}_{mb0} can be calculated from equation (A4).

Formula (A8) together with the solution of equation (A1)

$$M = M_0 + m \quad (\text{A9})$$

describe the evolution of A as a function of the amount of the accreted rest mass m .

REFERENCES

- Abramowicz M.A. & Lasota J.-P., 1980, *Acta Astron.*, 30, 35
- Belczyński K., Taam R.E., Rantsiou E., van der Sluys M., *ApJ* in press (astro-ph/0703131)
- Blandford R.D. & Znajek R.L., 1977, *MNRAS*, 179, 433
- Blandford, R. D. & Payne, D. G. 1982, *MNRAS*, 199, 883
- Contopoulos, J. 1995, *ApJ*, 450, 616
- Detmers R.G., Langer N., Podsiadlowski P., Izzard R.G., 2008, *Astronomy & Astrophysics*, in press
- Di Matteo T., Perna R., Narayan R., 2002, *ApJ*, 579, 706
- Gammie C.F., Shapiro S.L., McKinney J.C., 2004, *ApJ*, 602, 312
- Heger A., Woosley S.E., Spruit H., 2005, *ApJ*, 626, 350
- Janiuk A., Perna R., Di Matteo T., Czerny B., 2004, *MNRAS*, 355, 950
- Janiuk A., Yuan Y.-F., Perna R., Di Matteo T., 2007, *ApJ*, 664, 1011
- Janiuk A., Proga D., 2008, *ApJ*, 675, 519
- King A.R., Pringle J., 2006, *MNRAS*, 373, L90
- Lazzati D., 2005, *MNRAS*, 357, 722
- MacFadyen A.I., Woosley S.E., 1999, *ApJ*, 524, 262
- McKinney J.C., 2005, *ApJ*, 630, L5
- McBreen S., et al., 2006, *A&A*, 455, 433
- Mochkovitch R., Hernanz M., Isern J., Martin X., 1993, *Nature*, 361, 236
- Moderski R., Sikora M., 1996, *MNRAS*, 283, 854
- Moderski R., Sikora M., Lasota J.-P., 1998, *MNRAS*, 301, 142
- Morsony B.J., Lazzati D., Begelman M.C., 2007, *ApJ*, 665, 569
- Murakami T., Inoue H., Nishimura J., van Paradijs J., Fenimore E. E., 1991 *Nature*, 350, 592
- Paczynski, B., 1998, *ApJ*, 494, L45
- Perna R., Armitage P.J., Zhang B., 2006, *ApJ*, 636, L29
- Piro L., et al., 2005, *ApJ*, 623, 314
- Popham R., Woosley S.E., Fryer C., 1999, *ApJ*, 518, 356
- Pringle J. E., 1981, *ARA&A*, 19, 137
- Proga D., MacFadyen A.I., Armitage, P.J., Begelman, M.C., 2003, *ApJ*, 599, L5
- Racusin, J.L., et al., 2008, *Nature*, submitted (arXiv:0805.1557v1)
- Ramirez-Ruiz E., MacFadyen A.I., Lazzati D., 2002, *MNRAS*, 331, 197
- Romano et al., 2006, *A&A*, 456, 917
- Umeda H., Tominaga N., Maeda K., Nomoto K., 2005, *ApJ*, 633, L17
- Wang X.-Y. & Meszaros P., 2007, *ApJ*, 670, 1247
- Woosley S.E., 1995, *ApJ*, 405, 273
- Woosley S.E., Weaver T.A., 1995, *ApJS*, 101, 181
- Yoon S.-C., Langer N., Norman C., 2006, *A&A*, 460, 199

This 2-column preprint was prepared with the AAS L^AT_EX macros v5.2.